optimized characteristics have further been improved by addition of simple external circuits to bring forth much wider bandwidth.

### ACKNOWLEDGMENT

The authors thank H. J. Pang and T. Anada of Kanagawa University for their help in manufacturing the circuits used in the experiment.

### REFERENCES

[1] G. L Matthaei, L. Young, and E. M. T. Jones, *Microwave Filters, Impedance-Matching Networks and Coupling Structures*. New York: McGraw Hill, 1964, ch. 13.
[2] T. Okoshi and T. Miyoshi, "The planar circuit—An approach to microwave integrated circuitry," *IEEE Trans. Microwave Theory Tech.*, vol. MTT-20, pp. 245–252, Apr. 1972.
[3] T. Okoshi, Y. Uehara, and T. Takeuchi, "The segmentation method —An approach to the analysis of microwave planar circuits," *IEEE Trans. Microwave Theory Tech.*, vol. MTT-24, pp. 662–668, Oct. 1976.
[4] E. Polak, "Computational methods in optimization," in Mathematics in Science and Engineering Ser., vol. 77, New York: Academic, 1971.
[5] G. P. Riblet, "An eigenadmittance condition applicable to symmetrical four-port circulators and hybrids," *IEEE Trans. Microwave Theory Tech.*, vol. MTT-26, pp. 275–279, Apr. 1978, p. 277.
[6] N. Marcuvitz, "Waveguide Handbook, New York: McGraw Hill, 1951, sect 3.5.
[7] For example, R. F. Collin, "Field theory of guided waves," New York: McGraw Hill, 1960, Sect. 4.3.
[8] G. P Riblet, "A directional coupler with very flat coupling," *IEEE Trans. Microwave Theory Tech.*, vol. MTT-26, pp. 70–74, Feb. 1978.
[9] K. Grüner, "Method of synthesizing nonuniform waveguides," *IEEE Trans. Microwave Theory Tech* , vol MTT-22, pp 317–322, Mar. 1974.
[10] F. Kato, M. Saito, and T. Okoshi, "Computer-aided synthesis of planar circuits," *IEEE Trans. Microwave Theory Tech.*, vol. MTT-25, pp. 814–819, Oct. 1974.

# The Sector Coupler—Theory and Performance

JOHN W. ARCHER, MIKIO OGAI, MEMBER, IEEE, AND ERNEST M. CALOCCIA, MEMBER, IEEE

***Abstract*— The "sector coupler" is a practical, broad-band power divider for overdimensioned, millimeter-wavelength, $TE_{[01]}$ mode circular waveguide communications systems. The simple mechanical construction of the device, together with its very low insertion loss, high return loss, and low higher order $TE_{[0n]}$ mode coupling in the main line, make it ideally suited to applications where many devices must be installed in a long waveguide run.**

## I. INTRODUCTION

THE MILLIMETER-wavelength $TE_{[01]}$ mode circular waveguide system, installed at the site of the very large array (VLA) in central New Mexico, carries information modulated onto a millimeter-wavelength carrier in the frequency range 26.4 to 52 GHz between the many antennas in the array and the central Control Building [1], [2]. A single, low-loss, 60-mm diameter, helix-lined circular waveguide line is installed, running the full length of each arm of the array. Broad-band power dividers are installed in the main waveguide line at each antenna station to couple power to and from the main guide. The antenna waveguide system is comprised of approximately 40 m of 20-mm-diameter helix-lined circular waveguide, which includes rotary joints, rigid and flexible waveguide sections, connected to a transmit/receive modem operating within any given 1-GHz bandwidth channel in the 26.4- to 52-GHz range.

The coupling values required may vary between $-23$ and $-10$ dB, depending upon the transmission frequency and the distance from the central Control Building to the antenna station. However, because the spatial distribution of stations for optimum array configurations results in a greater number of stations within a relatively short distance from the Control Building, the coupling required at most locations is less than $-20$ dB. The devices exhibit very low return loss and higher order $TE_{[0n]}$ mode coupling in the forward and reverse directions in the main line, in order to minimize amplitude and phase distortion of the primary $TE_{[01]}$ mode transmission response. Furthermore, since no repeaters are used in the communication system, with 23 power dividers installed over the 20-km length of line, the magnitude of the $TE_{[01]}$ mode insertion loss of each device also has a significant impact on system performance.

With respect to the coupled port, when transmitting power from an antenna into the trunk waveguide, both the

Manuscript received July 22, 1980; revised September 25, 1980. The National Radio Astronomy Observatory is operated by Associated Universities, Incorporated, under Contract with the National Science Foundation.

J. W. Archer is with the National Radio Astronomy Observatory, Charlottesville, VA 22903.
M. Ogai was with the National Radio Astronomy Observatory, Socorro, NM. He is now with Furukawa Cable Co., Tokyo, Japan.
E. M. Caloccia was with the National Radio Astronomy Observatory, Socorro, NM. He is now with Raytheon, Inc., Missile Systems Division, Bedford, MA 01730.

0018-9480/81/0300-0202$00.75 

$TE_{[01]}$ mode reflection coefficient and the $TE_{[10]}$ to $TE_{[0n]}$ mode coupling must be small, so as to minimize distortion of the $TE_{[01]}$ mode transfer function. A detailed discussion of these performance specifications is given by Weinreb *et al.* [1] and Archer *et al.* [2].

## II. The "Sector Coupler"—Physical Description

Consider an infinitesimally thin, perfectly conducting sheet placed perpendicular to the electric field lines of the $TE_{[0n]}$ modes in a diametrical plane of a waveguide of circular cross section. Then the electric field distribution of the $TE_{[0n]}$ modes remains unperturbed. In fact, any two such radial planes intersecting at the center line of the cylinder, with arbitrary included angle, also leave the electric field pattern unchanged.

Such a configuration can be said to result in the formation of a pair of "sector" waveguides, with the composite field pattern of the pair identical to that of the original circular waveguide. However, in these sector waveguides, only the characteristics of the $TE_{[0n]}$ and $TM_{(0n)}$ modes are similar to those of the corresponding modes in normal circular waveguide. Ideally, power in a $TE_{[0n]}$ mode incident on a transition from ordinary circular waveguide to the sector waveguide composite will propagate forward without reflection or mode conversion. The proportion of the incident power coupled into each sector waveguide is directly proportional to the ratio of the angles subtended by the sectors.

In the "sector coupler," power coupled to the sector waveguide of smaller subtended angle is fed to an external waveguide port, whereas power coupled to the larger sector is reconverted to the normal circular electric modes of the main waveguide by gradually tapering the angle subtended by the smaller sector to zero. Several methods can be devised to change the direction of signal flow in the smaller angle sector waveguide and couple the power to a third external waveguide port. Of these, the most physically compact for a given change in angle relative to the axis of the main guide (separation angle) employs a plane, perfectly conducting mirror in the sector waveguide to transform the incident field of one sector waveguide to that of a complementary one oriented at the desired separation angle. The sector $TE_{[01]}$ mode is then transformed to the semicircular guide $TE_{[01]}$ mode in an angular taper transition. Finally, power is reconverted to the circular $TE_{[01]}$ mode at an abrupt semicircular-to-circular junction in which the second semicircular port is terminated.

The complete concept is illustrated in Fig. 1. The evident mechanical simplicity of the device enables the manufacture of many units with repeatable performance characteristics. However, the straightforward mechanical design belies the complex nature of the electrical performance of the sector coupler. In order to explain the electrical behavior of the device, the abrupt sector-to-circular waveguide transition, the angular taper sector-to-semicircular transition, and the abrupt change in angular orientation of the sector waveguide at a reflecting surface in the guide must

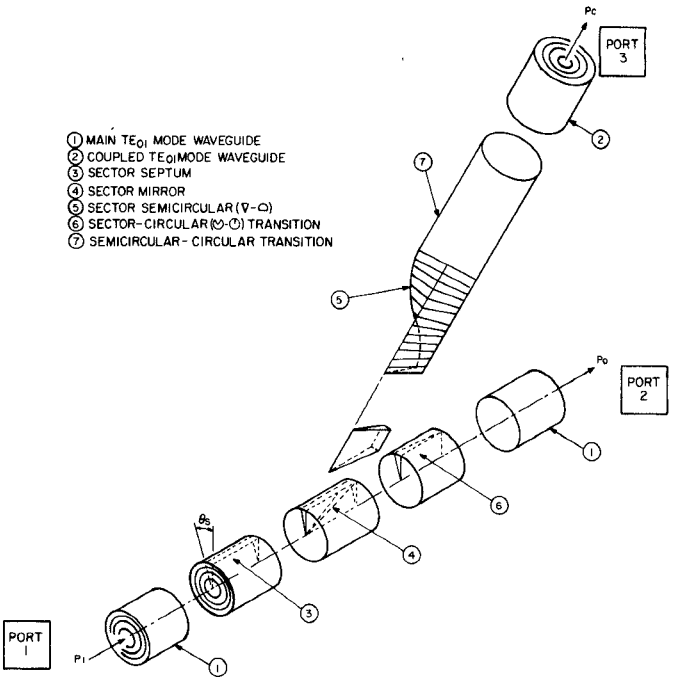


Fig. 1. The sector coupler concept.

be analyzed theoretically. An outline of the method of analysis is presented in the following section.

## III. Theoretical Analysis

### A. Abrupt Circular-to-Sector Waveguide Transition

The "sector coupler" is a power coupling device which operates in highly overmoded circular waveguide systems and, therefore, cannot be represented as a simple, single-mode, 3-port waveguide junction. The sector-to-circular transition must be treated as a multiport waveguide junction in which each port is considered as a terminal pair for one of the nonevanescent modes of the waveguide triplet forming the discontinuous structure. For practical reasons, consideration is usually restricted to the first $N$ modes, taken in order of cutoff wavelength, in each waveguide. The junction may then be approximated by a $3N$-port model. An analytical procedure for deriving the elements of the scattering matrix for the $3N$-port is outlined in the Appendix.

It will suffice, here, to demonstrate the basic properties of the sector-to-circular transition and to present the significant results of the theoretical analysis from the Appendix. Of principal interest in the operation of the practical sector coupler is the case where power is incident on the junction from one of the sector waveguide ports representing a $TE_{[0n]}$ mode. Specifically, label this port 1 and the corresponding $TE_{[0n]}$ mode ports for the complimentary sector and the circular waveguides 2 and 3, respectively. The complete scattering matrix of the $3N$-port junction may then be written as

$$\boldsymbol{S}=\left(\begin{array}{ccc|c} s_{11} & s_{12} & s_{13} & \\ s_{21} & s_{22} & s_{22} & \boldsymbol{T} \\ s_{31} & s_{32} & s_{33} & \\ \hline & \boldsymbol{V} & & \boldsymbol{U} \end{array}\right)$$

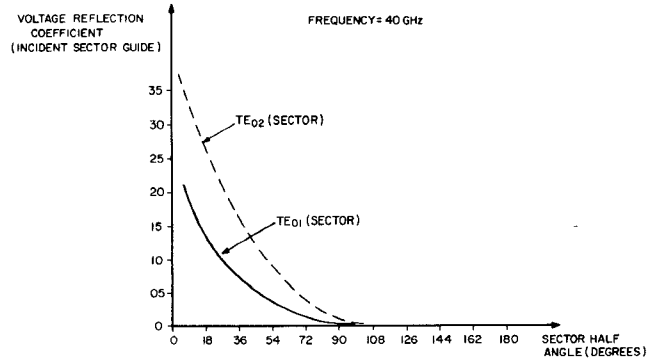


Fig. 2. Predicted reflection coefficient in the sector waveguide as an abrupt sector/circular transition, as a function of sector angle.

where the scattering parameters $s_{ij}$ relate the incident ($a_i$) and scattered ($b_j$) normalized, complex-valued, scalar wave amplitudes at ports $i$ and $j$, respectively. All ports other than port 1 will be considered to be terminated in an impedance equal to the wave impedance for the mode and relevant waveguide of the structure represented, i.e., the normalized incident wave amplitude at all other ports is zero. The scattering parameter submatrices $\boldsymbol{T}$ and $\boldsymbol{V}$ define the coupling between ports 1, 2, or 3 and all other $(3N-3)$-ports of the network. Submatrix $\boldsymbol{U}$ is the scattering matrix for the remaining $(3N-3)$-ports alone.

Since the device contains only material characterized by symmetric, scalar valued conductivity, permeability, and permittivity tensors the Lorentz reciprocity condition applies to the structure. The $3N$-port junction is, therefore, reciprocal [8] and

$$\boldsymbol{S}=\boldsymbol{S}^T$$

where $\boldsymbol{S}^T$ indicates the transpose of $\boldsymbol{S}$.

Furthermore, if the junction is formed from perfectly conducting material, the $3N$-port is also lossless, $\boldsymbol{S}$ is unitary and

$$\boldsymbol{S}\boldsymbol{S}^*=\boldsymbol{I}$$

where $\boldsymbol{S}^*$ indicates the complex conjugate of $\boldsymbol{S}$.

The values of the elements of the principal $3\times3$ submatrix of interest are derived in the Appendix. The diagonal elements are

$$s_{11}=\frac{1-\alpha}{1+\alpha} \qquad \text{(sector guide)}$$

$$s_{22}=\frac{1-\beta}{1+\beta} \qquad \text{(complimentary sector guide)}$$

$$s_{33}=0 \qquad \text{(circular guide)}$$

where $\alpha$ and $\beta$ are functions of the scattering parameters $s_{1i}$ $(i\neq1)$, $s_{2j}$ $(j\neq2)$, respectively.

The coefficients $s_{ii}$ for a sector guide are plotted in Fig. 2 as a function of sector angle for $TE_{[01]}$ and $TE_{[02]}$ modes incident at the transition.

The forward coupling parameters are given by

$$s_{13}=s_{31}=\sqrt{\frac{\psi}{2\pi}}$$

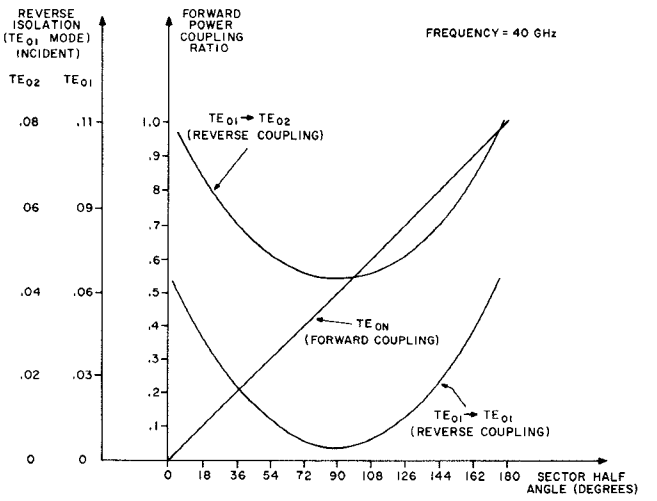


Fig. 3. Predicted $TE_{[0n]}$ mode coupling at a sector/circular waveguide transition, as a function of sector angle. Note that coupling from $TE_{[01]}$ (sector) to $TE_{[02]}$ (circular) is predicted to be negligibly small.

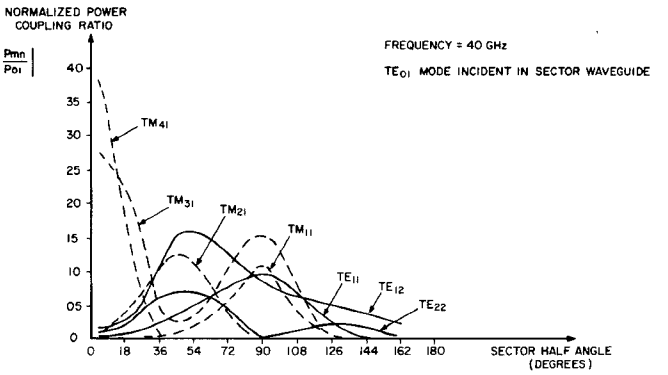


Fig. 4. Power coupled to some of the modes excited in the circular waveguide at an abrupt sector/circular transition, as a function of sector angle.

where $\psi$ is the angle included by the sector waveguide 1 corresponding to port 1, and

$$s_{32}=s_{23}=\sqrt{\frac{2\pi-\psi}{2\pi}}$$

for the complimentary sector guide.

The coupling between the sector waveguides (scattering parameters $s_{12}, s_{21}$) is plotted in Fig. 3, as a function of sector angle, for $TE_{[01]}$ and $TE_{[02]}$ modes incident. These results were obtained from a numerical solution of the mode-matching equations outlined in the Appendix. Simple closed-form solutions do not exist for this coupling parameter. For a $TE_{[0n]}$ mode, the curves show that the device is expected to exhibit finite isolation between the sector waveguides. The isolation increases as the sector angle subtended by the input waveguide increases from 0 to $\pi$. Since the device is reciprocal, for sector angles greater than $\pi$, the isolation equals that for the case where the sector angle is $2(\psi-\pi)$. It can be seen from Fig. 3 that the junction is predicted to exhibit directional properties ($s_{12} < s_{13}, s_{23}$).

Fig. 4 presents a selection of additional results of the

numerical analysis, showing the predicted mode coupling for a $TE_{[01]}$ mode incident from a sector waveguide of given included angle to other nonsymmetric $TE_{[mn]}$ and $TM_{(mn)}$ modes in the circular waveguide. A first-order solution for these coefficients is derived in the Appendix.

It may be concluded from the foregoing results that the "sector coupler" cannot strictly be described as a $TE_{[0n]}$ mode directional coupler, in that it exhibits finite isolation and is intrinsically mismatched when those modes are incident. However, since the device is reciprocal, exhibits nonzero directivity, and possesses acceptably small return loss for $TE_{[0n]}$ modes at all three waveguide inputs, it may, in practice, be considered to approximate the behavior of a directional coupler in most respects when used in a helix-lined waveguide system.

### *B. The Angular Taper Sector-to-Circular Transition*

In the coupled arm of the device, incident power in the sector $TE_{[01]}$ mode is first reconverted to the semicircular $TE_{[01]}$ mode and then to the circular $TE_{[01]}$ mode at an abrupt sector/circular transition in which the complementary sector waveguide is terminated. The change in sector angle may be accomplished by changing the angle linearly as a function of axial distance. A sector angle transducer of this nature, while relatively simple to fabricate, results in mode conversion between $TE_{[0n]}$ modes and numerous higher order $TE_{[mn]}$ and $TM_{(mn)}$ $(m \neq 0)$ modes. As a consequence, the $TE_{[0n]}$ mode loss through the transition is greater than that due to copper losses alone if the power in the spurious modes is subsequently dissipated in a length of helix-lined waveguide.

To predict the magnitude of the mode-coupling coefficients from $TE_{[01]}$ to $TE_{[mn]}$ and $TM_{(mn)}$ modes in this kind of transition requires first that Maxwell's equations be expressed in oblique coordinates, which is the natural system for a helix taper. Expressing the transverse electric and magnetic fields of the sector waveguide in terms of the normal mode functions $T_{[mn]}$, $T_{(mn)}$, inhomogeneous second-order linear differential equations may be obtained relating the amplitudes of the $TE_{[01]}$ and $TE_{[mn]}$, $TM_{(mn)}$ modes in the angular taper [3], [7]. To achieve a solution, reciprocity is invoked, so that, in fact, coupling from an incident $TE_{[mn]}$ or $TM_{(mn)}$ mode to the $TE_{[01]}$ modes is calculated. Furthermore, the power of the incident modes is assumed to be constant along the taper (or alternatively, the coupling to secondary modes is assumed to be weak) and conversion–reconversion mechanisms are neglected.

If the angular taper is described by the equation

$$\Phi = \frac{z}{T}$$

where $\Phi$ is the sector half angle at axial position $z$, then formulas expressing the mode-coupling coefficients as integrals over the axial length of the taper may be obtained [3], [7].

The resulting integrals were evaluated numerically to give the coupling coefficients between either the $TE_{[01]}$ or

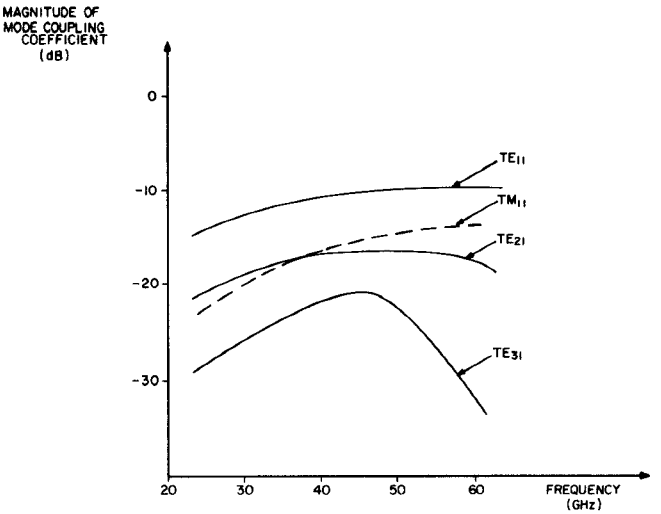


Fig. 5. Mode coupling in a sector/semicircular angular taper transition. Initial sector angle 9°, $T=0.1612$ m/rad, $TE_{[01]}$ mode incident.

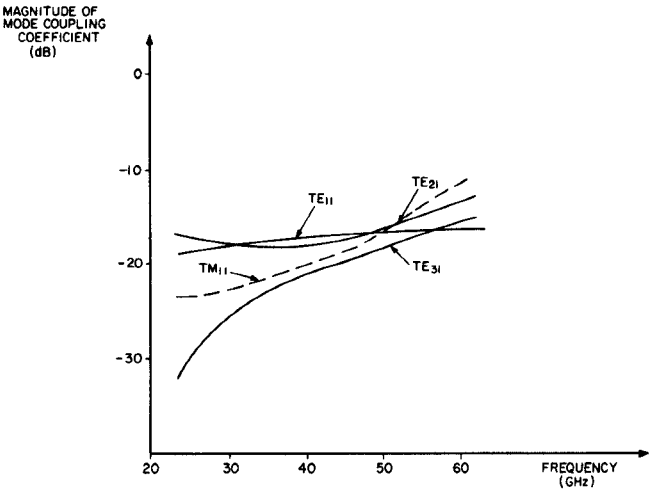


Fig. 6. Mode coupling in a sector/semicircular angular taper transition. Initial sector angle 9°, $T=0.1612$ m/rad, $TE_{[02]}$ mode incident.

$TE_{[02]}$ modes and the $TE_{[11]}$, $TE_{[21]}$, $TE_{[31]}$, and $TM_{(11)}$ modes as a function of frequency and initial sector angle, for tapers to 180°, with $T=0.1612$ m/rad. The results of these computations are presented graphically in Figs. 5 and 6. These curves enable the excess $TE_{[01]}$ mode insertion loss of the transition, due to mode coupling, to be predicted.

### *C. Sector Waveguide Corner Reflector*

Power coupled to the sector waveguide from the main trunk waveguide undergoes an abrupt change in direction at a plane, perfectly reflecting surface, as shown in Fig. 1. The incident electromagnetic fields of the sector waveguide are transformed at the junction to the fields of a complementary guide oriented at the desired separation angle. Although experimental measurements indicate that this type of junction possesses low $TE_{[01]}$ mode insertion loss and acceptably small $TE_{[01]} \rightarrow TE_{[02]}$ mode coupling, the

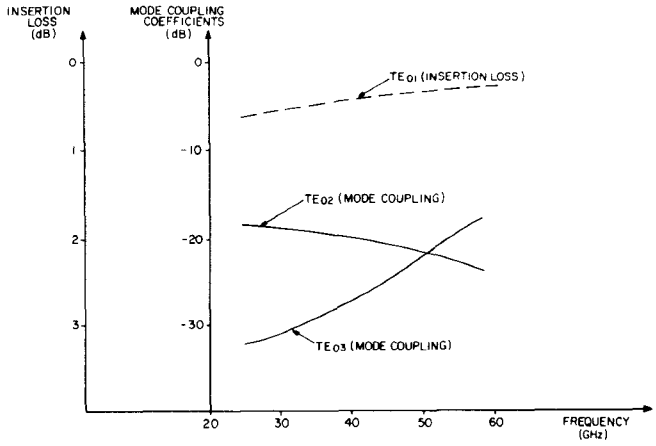


Fig. 7. Predicted mode coupling coefficients for the sector waveguide corner reflector transition with $TE_{[01]}$ mode incident. Separation angle 90°, sector angle 9°.

very complex boundary conditions for the fields in the vicinity of the reflecting surface preclude an exact analysis. Furthermore, the approximate analytical methods used by Marcatili [6] in analyzing the geometrically similar problem of a circular waveguide corner reflector cannot be applied here because of a lack of symmetry in the sector waveguide structure.

An attempt to formulate an analytical approach to the problem of the sector waveguide corner reflector using the results of antenna theory is outlined briefly below. The analysis gave results which are in general agreement with experimental data, even though gross simplifying approximations were made in specifying the boundary conditions at the reflecting surface. The approximate current distribution at the corner reflector surface and at the sector waveguide walls due to the field in the input waveguide was first evaluated. Then the contributions to the scalar aperture field of the output sector guide, by direct radiation from the input sector waveguide aperture and radiation from each boundary surface, were calculated independently and the resultant total field obtained by superposition. The computer analysis commenced with the assumption that the transverse fields in the aperture of the sector waveguide from which power was incident were those of the $TE_{[01]}$ mode. The surface current distributions were then calculated and the integrations for the resultant output field performed numerically.

Mode coupling at the junction was analyzed by expressing the derived normalized field distribution as a linear combination of normal mode functions for the $TE_{[0n]}$ modes in sector waveguide, with $\phi=0$. The coefficients of this series can be used to predict the magnitude of the coupling from $TE_{[01]}$ to $TE_{[0n]}$ modes in the corner waveguide junction. This method clearly neglects possible coupling to other $TE_{[mn]}$ and $TM_{(mn)}$ modes. However, the nature of field distributions derived for $\phi\neq 0$ suggests that coupling to these modes is small compared to $TE_{[01]}$ to $TE_{[0n]}$ mode interactions, at least to the order of the approximations made in the analysis. Fig. 7 shows predicted $TE_{[01]}$ to $TE_{[0n]}$ mode insertion loss at the junction due to mode coupling losses.

## IV. Predicted and Measured Performance

### A. Predictions of the Performance Characteristics

The behavior of the complete "sector coupler" may be predicted on the basis of the foregoing theoretical analysis of the component parts of the device. The significant aspects of device performance and the relevant theoretical considerations are outlined below. Figs. 8 and 9 illustrate the predicted and experimental dependence of these performance parameters on frequency and also their relationship to principal sector angle ($2\psi$; $\psi<\pi/2$) at a frequency of 40 GHz.

*1) $TE_{[01]}$ Mode Main Line Insertion Loss and Return Loss:* The main line insertion and return loss may be predicted for a given device on the basis of the analysis of the abrupt sector-to-circular waveguide transition. A small direction dependence is predicted in these parameters depending upon which port is considered the input. This results from direction-dependent variation in coupling losses and reflection coefficients at the sector-to-circular waveguide interface.

*2) $TE_{[01]}$ Mode Coupling Loss and Directivity for the Coupled Port:* The coupling loss is influenced by three mechanisms in the "sector coupler." The sector angle ratio is the principal determinant of coupling for a given coupler. Additional losses are contributed by the sector waveguide corner reflector, sector-to-semicircular angular taper transition, and the abrupt semicircular-to-circular waveguide junction in the coupled arm. Directivity, however, depends principally upon the geometry of the abrupt sector-to-circular waveguide transition in the main trunk waveguide.

*3) $TE_{[01]}$ to $TE_{[0n]}$ Mode Coupling in the Coupled Arm:* Interactions between circular electric modes in the coupled arm of the device can be considered to result from two mechanisms. The principal source of direct coupling is, as predicted theoretically, the sector waveguide corner junction. However, the experimental results indicate that the coupled arm mode coupling response exhibits a quasi-periodic variation (of small amplitude) about a nominal coupling value. The nonuniformity in the coupling response is thought to arise from second-order mode coupling ($TE_{[02]}\rightarrow[TE_{[mn]}, TM_{(mn)}]\rightarrow TE_{[01]}$) in the sector-to-semicircular waveguide angular taper, since results for different taper lengths (different taper constant) indicate that the effect is greater, and the periodicity larger, for short tapers, in which the general level of mode coupling is higher. The approximate theoretical analysis of Section III-B neglected secondary conversion–reconversion mechanisms and thus could not predict the observed effect. For a taper length of 0.24 m the coupling mechanism due to secondary interactions may be approximated by a $TE_{[01]}$ to $TE_{[02]}$ mode coupling discontinuity with coupling coeffi-

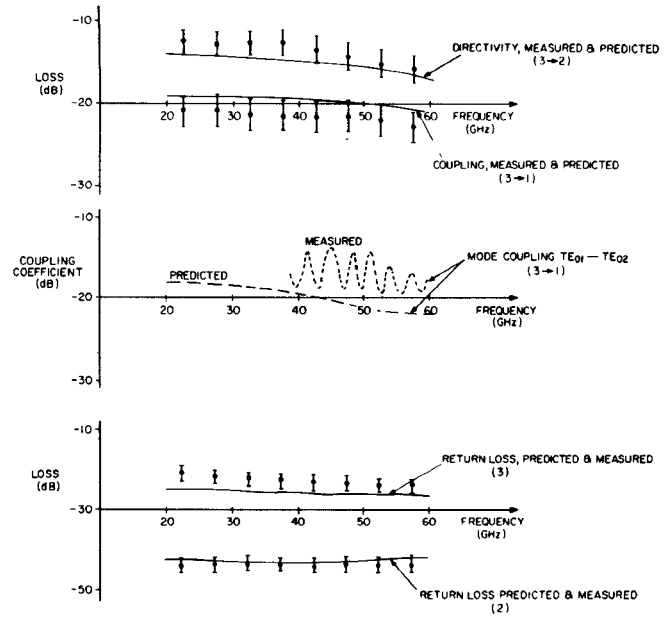


Fig. 8. Comparison of predicted and measured performance of a large sample of sector couplers with sector angle of 9°. Main line insertion loss (ports 1→2) is less than 0.15 dB between 26.5 and 60 GHz. Numbers in brackets identify coupler ports concerned with the given parameter (refer to Fig. 1).

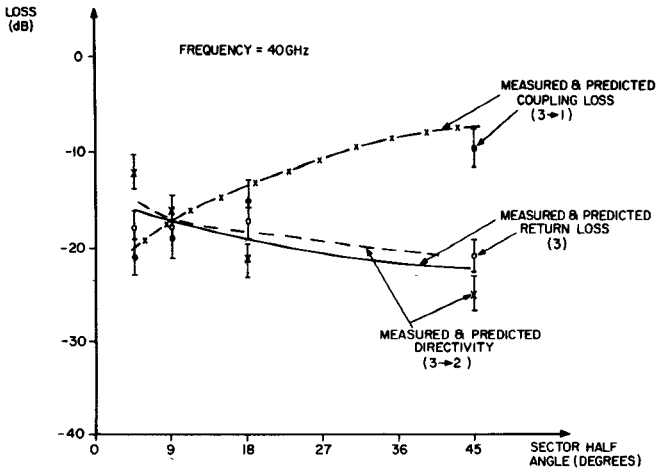


Fig. 9. Some sector coupler performance parameters plotted as a function of sector half angle.

cient −10 dB located approximately 0.20 m from the sector waveguide corner reflector junction.

*4) $TE_{[01]}$ Mode Return Loss in the Coupled Arm:* For power incident at the coupled arm of the device, the principal source of reflection is the abrupt sector-to-circular transition in the main waveguide. The incident and reflected signals are modified by the additional losses in the coupled arm signal path as outlined in 2), resulting in a significantly better return loss at the input to the coupled port than would be predicted due to $TE_{[01]}$ mode reflections at the abrupt transition alone.

*5) $TE_{[0n]}$ Mode Generation in the Main Line:* For power incident from either of the main trunk waveguide ports, higher order circular TE mode coupling is, in general, very small, as predicted by the analysis outlined in Section III-A. For power incident from the coupled port, forward coupling to higher order modes in the main circular waveguide is also negligible. However, the theory predicts a small, but significant, reverse coupling of higher order modes into the complementary sector waveguide.

### *B. Measured Performance Statistics*

More than sixty "sector couplers," with varying degrees of coupling, have been fabricated, tested, and installed in the waveguide communication system at the VLA site. The measured points shown in Figs. 8 and 9, therefore, represent mean performance of a large sample of devices. The error bars in the figure denote the peak deviation from the mean of a given performance measure over the sample space. Experimental errors have been assumed negligible compared with the scatter in performance of such a large sample of couplers. It can be seen that the theoretically predicted behavior is in reasonable agreement with the measured performance. The fact that the theoretical treatment neglects copper losses in the waveguides possibly accounts for the small discrepancies between predicted and measured loss values. Clearly, the "sector coupler" behavior is sufficiently well understood theoretically to enable the effects of the variables in the design to be adequately evaluated.

## V. Conclusion

An analytical approach to the evaluation of a novel type of power divider for overdimensioned circular waveguide has been outlined. Adequate agreement between theory and experiment has been demonstrated. The power dividers are of mechanically simple construction, yet exhibit very low insertion loss, high return loss, and low higher order $TE_{[0n]}$ mode coupling in the main line. These performance characteristics as well as the broad constant-coupling bandwidth make the "sector coupler" ideally suited to applications in broad-band waveguide communications systems where many devices must be installed in the waveguide line.

## Appendix

### Mode Coupling at a Sector-to-Circular Waveguide Junction

The mode-conversion coefficients at a sector-to-circular transition, with a $TE_{[0n]}$ mode incident from one of the sector waveguides, may be derived by considering field continuity constraints at the junction [4]. Sets of $N+1$ linear equations may be obtained which describe the coupling to $N$ modes in the circular waveguide ($B$). The pair of sector waveguides may be thought of as forming a composite waveguide ($A$) with $N$ individual modes defined over each sector aperture only—a total of $2N$ modes for the composite. Let the mode amplitudes in $A$ have amplitude coefficients $a_i$, $i=1,\cdots,2N$, where $i=1$ corresponds

to the $TE_{[0n]}$ mode incident. Similarly, let mode amplitudes in $B$ be represented by $b_i$, $i=1,\cdots,N$. Then the continuity conditions for the electric and magnetic fields may be expressed as

$$(1+R)a_2\boldsymbol{e}_1+\sum_{i=1}^{2N}a_i\boldsymbol{e}_i=\sum_{j=1}^{N}b_j\boldsymbol{e}_j^{(t)} \tag{1}$$

$$(1-R)a_1\boldsymbol{h}_1-\sum_{i=1}^{2N}a_i\boldsymbol{h}_i=\sum_{j=1}^{N}b_j\boldsymbol{h}_j^{(t)} \tag{2}$$

where

$R$ is the reflection coefficient for mode 1 in waveguide $A$;

$\boldsymbol{e}, \boldsymbol{h}$ represent the electric and magnetic field mode functions in the composite waveguide $A$ [3];

$\boldsymbol{e}^{(t)}, \boldsymbol{h}^{(t)}$ represent the mode functions in waveguide $B$.

Let $Y_i, Y_i^{(t)}$ be the wave admittance for the $i$th mode in waveguides $A$ and $B$, respectively.

Take the cross product of (1) with $\boldsymbol{h}_k$ or $\boldsymbol{h}_1^{(t)}$ and integrate over the cross section of the composite guide $B$ or $A$, respectively, then the cross product of (2) with $\boldsymbol{e}_k$ or $\boldsymbol{e}_1^{(t)}$ and perform similar integrations, resulting in the equations

$$(1+R)\Phi_{11}=\sum_{j=1}^{N}\frac{b_j}{a_1}\phi_{j1}$$

$$(1-R)\Phi_{11}=\sum_{j=1}^{N}\frac{Y_j^{(t)}}{Y_1}\frac{b_j}{a_1}\phi_{j1}$$

$$(1+R)\frac{Y_n^{(t)}}{Y_1}\phi_{n1}-\sum_{j=1}^{N}\sum_{i=2}^{2N}\frac{Y_j^{(t)}}{Y_i}\cdot\frac{Y_n^{(t)}}{Y_i}\cdot\frac{b_j}{a_1}\cdot\frac{\phi_{ji}\phi_{ni}}{\Phi_{ii}}=\frac{b_n}{a_1}\Phi'_{nn}$$

$$(1-R)\phi_{n1}-\sum_{j=1}^{N}\sum_{j=2}^{2N}\frac{b_j}{a_1}\frac{\phi_{ji}\phi_{ni}}{\Phi_{ii}}=\frac{b_n}{a_1}\Phi'_{nn}$$

$$\frac{a_i}{a_1}=\sum_{j=1}^{N}\frac{\frac{b_j}{a_1}\phi_{ji}}{\Phi_{ii}}=-\sum_{j=1}^{N}\frac{\frac{b_j}{a_1}\frac{Y_j^{(t)}}{Y_i}\phi_{ji}}{\Phi_{ii}}$$

where

$$\phi_{ij}=\int_A \boldsymbol{e}_i^{(t)}\times\boldsymbol{h}_j\cdot\boldsymbol{u}_z\,ds$$

$$\Phi_{ii}=\int_A \boldsymbol{e}_i\times\boldsymbol{h}_i\cdot\boldsymbol{u}_z\,ds$$

$$\Phi'_{ii}=\int_B \boldsymbol{e}_i^{(t)}\times\boldsymbol{h}_i^{(t)}\cdot\boldsymbol{u}_z\,ds.$$

These equations have been solved numerically for the coefficients $R$, $b_j/a_1$, $a_i/a_1$. The integrals do not, in general, possess closed-form solutions and were evaluated numerically [5]. Several interesting results may be obtained from these equations.

*1) $TE_{[0n]}$ Forward Coupling (Sector 1 to Circular Waveguide):*

$$\frac{b_1}{a_1}=\frac{\phi_{11}}{\Phi'_{11}}-\frac{1}{\Phi'_{11}}\sum_{j=1}^{N}\frac{b_j}{a_1}\sum_{i=2}^{2N}\frac{\phi_{ji}\phi_{1i}}{\Phi_{ii}}\left(1+\frac{Y_j^{(t)}Y_1}{Y_i^2}\right)$$

but

$$\phi_{1i}=0, \qquad \text{if } i\neq 1$$

hence

$$\frac{b_1}{a_1}=\frac{\phi_{11}}{\Phi'_{11}}=\sqrt{\frac{\psi}{\pi}}\,.$$

*2) First-Order Solution for Coupled Modes (In Sectors 1 and 2 and Circular Guide):*

Zeroth order:

$$\frac{b_j}{a_1}^{(0)}=\frac{2}{1+\frac{Y_j^{(t)}}{Y_1}}\frac{\phi_{j1}}{\Phi'_{jj}}.$$

First order:

$$\frac{a_i}{a_1}^{(1)}=\sum_{j=1}^{N}\frac{2}{1+\frac{Y_j^{(t)}}{Y_1}}\frac{\phi_{j1}}{\Phi'_{jj}}\cdot\phi_{ji}$$

$$\frac{b_j}{a_1}^{(1)}=\frac{2}{1+\frac{Y_j^{(t)}}{Y_1}}\left(\frac{\phi_{j1}}{\Phi'_{jj}}+\frac{1}{2}\sum_{i=1}^{2N}\frac{b_j}{a_1}^{(0)}\left(1-\frac{Y_j^{(t)}}{Y_i}\right)\frac{\phi_{ji}}{\Phi_{ii}}\right).$$

*3) Reflection Coefficient for $TE_{[0n]}$ Mode in Sector 1:*

$$\frac{1-R}{1+R}=\sum_{j=1}^{N}\frac{Y_j^{(t)}}{Y_1}\frac{b_j}{a_1}\cdot\frac{\phi_{j1}}{\sum_{k=1}^{N}\frac{b_k}{a_1}\phi_{k1}}.$$

## References


[1] S. Weinreb, R Predmore, M. Ogai, and A. Parrish, "Waveguide system for a very large antenna array," *Microwave J.*, vol. 20, no. 3, pp. 49–52, Mar 1977

[2] J W Archer, E. M. Caloccia, and R. Serna, "An evaluation of the performance of the VLA circular waveguide system," *IEEE Trans. Microwave Theory Tech.*, vol. MTT-28 pp. 786–791, July 1980.

[3] S. Iiguchi, "Mode conversion in the excitation of $TE_{01}$ waves in a $TE_{01}$ mode transducer," in *Proc. Symp. MM-Waves* (Polytechnic Instit., Brooklyn, Apr 1–2, 1959), p. 595.

[4] A. Wexler, "Solution of waveguide discontinuities by modal analysis," *IEEE Trans. Microwave Theory Tech*, vol. MTT-15, no 9, pp. 508–517, Sept. 1967

[5] G. Fairweather, "Modified Romberg quadrature," in *Comm. ACM 12*, p. 324, June 1969.

[6] E. A. J. Marcatili, "Miter elbow of circular electric mode," in *Proc. Symp. on Quasioptics* (Polytechnic Instit., Brooklyn, June 1964), p. 535.

[7] F Sporleder and H.-G. Unger, *Waveguide Tapers, Transitions and Couplers* (IEEE Electromagnetic Wave Series, no. 6). London, England: 1979, ch 7.

[8] K Kurokawa, *An Introduction to the Theory of Microwave Circuits* New York: Academic Press, 1969, ch. 5, p. 219.